

# Distinct Transcription Profiles of Primary and Secondary Glioblastoma Subgroups

Cho-Lea Tso,<sup>1,2,6</sup> William A. Freije,<sup>1</sup> Allen Day,<sup>1</sup> Zugen Chen,<sup>1</sup> Barry Merriman,<sup>1</sup> Ally Perlina,<sup>1</sup> Yohan Lee,<sup>1</sup> Ederlyn Q. Dia,<sup>3</sup> Koji Yoshimoto,<sup>3</sup> Paul S. Mischel,<sup>3,6</sup> Linda M. Liau,<sup>4,6</sup> Timothy F. Cloughesy,<sup>5,6</sup> and Stanley F. Nelson<sup>1,6</sup>

Departments of <sup>1</sup>Human Genetics, <sup>2</sup>Medicine/Hematology-Oncology, <sup>3</sup>Pathology and Laboratory Medicine, <sup>4</sup>Neurosurgery, and <sup>5</sup>Neurology, David Geffen School of Medicine, and <sup>6</sup>Jonsson Comprehensive Cancer Center, University of California at Los Angeles, Los Angeles, California

## Abstract

**Glioblastomas are invasive and aggressive tumors of the brain, generally considered to arise from glial cells. A subset of these cancers develops from lower-grade gliomas and can thus be clinically classified as “secondary,” whereas some glioblastomas occur with no prior evidence of a lower-grade tumor and can be clinically classified as “primary.” Substantial genetic differences between these groups of glioblastomas have been identified previously. We used large-scale expression analyses to identify glioblastoma-associated genes (GAG) that are associated with a more malignant phenotype via comparison with lower-grade astrocytomas. We have further defined gene expression differences that distinguish primary and secondary glioblastomas. GAGs distinct to primary or secondary tumors provided information on the heterogeneous properties and apparently distinct oncogenic mechanisms of these tumors. Secondary GAGs primarily include mitotic cell cycle components, suggesting the loss of function in prominent cell cycle regulators, whereas primary GAGs highlight genes typical of a stromal response, suggesting the importance of extracellular signaling. Immunohistochemical staining of glioblastoma tissue arrays confirmed expression differences. These data highlight that the development of gene pathway-targeted therapies may need to be specifically tailored to each subtype of glioblastoma.** (Cancer Res 2006; 66(1): 159-67)

## Introduction

Human solid tumors undergo multiple genetic evolutionary abnormalities as they evolve from normal cells to early-stage tumors to aggressive cancers (1). Chromosome instability that results in the development of both numerical abnormalities (aneuploidy) and structural abnormalities (chromosomal breakage, deletions, and amplification) is especially striking in many types of solid tumors (1, 2). A series of genome-wide chromosomal imbalance analyses and multiparameter cell-based studies suggest that genomic changes that lead to the loss of tumor suppressor gene function usually occur at early stages, whereas the later stages often involve the accumulation of multiple gain-of-function abnormalities that confer on tumors the potential for malignant transformation (3, 4). It

is possible that the malignant end points that are ultimately reached will prove to be shared in common by many types of tumors (5). The identification and functional assessment of genes altered in the process of malignant transformation is essential for understating the mechanism of cancer development and should facilitate the development of more effective treatments.

Infiltrative astrocytic neoplasms are the most common brain tumors of central nervous system in adults. Glioblastoma multiforme (WHO grade IV) remains a devastating disease, with a median survival of <1 year after diagnosis (6). Glioblastomas are defined by histopathologic features of cellular atypia, mitotic figures, necrotic foci with peripheral cellular pseudopalisading, and microvascular hyperplasia that distinguish it from lower-grade astrocytic tumors (7). Two subgroups of glioblastomas have been established based on clinical experience and have been affiliated with distinct genetic mechanisms of tumorigenesis. Secondary glioblastomas develop slowly through progression from low-grade glial tumors (WHO grade II) or anaplastic glial tumors (WHO grade III) and frequently contain mutations in the *p53* gene (~60%), overexpression of platelet-derived growth factor receptors, and loss of heterozygosity (LOH) at 17p, 19q, and 10q (8, 9). In contrast, primary glioblastomas seem to develop rapidly and manifest high-grade lesion from the outset and are genetically characterized by amplification/overexpression of epidermal growth factor receptor (EGFR; ~60%) and mouse double minute 2 (~50%), PTEN mutations, and loss of all or a portion of chromosome 10 (8, 9).

The objective of this study was to identify gain-of-function genes that are associated with acquisition of malignant features of glioblastomas. In addition, we investigated whether clinically defined primary and secondary glioblastoma subgroups use distinct molecular pathways. DNA microarray experiments were done to establish a transcription database for 101 glial brain tumors for which clinical and pathologic features as well as biopsy material were available. Through a series of comparative analyses against lower-grade astrocytomas, we have identified shared and distinct gene categories of transcripts overexpressed in glioblastoma subgroups that are associated with malignant transformation. The distinct glioblastoma-associated genes (GAG) further led to the discovery of stromal/mesenchymal properties in glioblastoma subgroup.

## Materials and Methods

**Tumor sample and data collection.** The patient tumors and normal samples were collected either from autopsies of glioblastoma patients within 24 hours of death or from patients who underwent surgery at University of California at Los Angeles (UCLA) Medical Center. All samples were collected under protocols approved by the UCLA Institutional Review Board. All histopathologic typing and tumor grading

**Note:** Supplementary data for this article are available at Cancer Research Online (<http://cancerres.aacrjournals.org/>).

**Requests for reprints:** Stanley F. Nelson, Department of Human Genetics, David Geffen School of Medicine, University of California at Los Angeles, Room 5506, 695 Young Drive South, Los Angeles, CA 90095. E-mail: [sfnelson@mednet.ucla.edu](mailto:sfnelson@mednet.ucla.edu).

©2006 American Association for Cancer Research.

doi:10.1158/0008-5472.CAN-05-0077

was done by one neuropathologist (P.S.M.) according to the WHO criteria (10). The subgrouping of glioblastomas was based on clinical presentation. Secondary glioblastomas were called if there was previous pathologic evidence of lower-grade glioblastomas. All tumors without prior evidence of progression from a lower-grade tumor were clinically classified as primary glioblastomas. All samples were snap frozen in liquid nitrogen and stored at  $-80^{\circ}\text{C}$  before being processed for the microarray and reverse transcription-PCR (RT-PCR) analyses. Some of the data presented here are derived from a published microarray study (11). Among the data available from the Freije et al. article (11), 43 clinical grade IV glioblastomas were selected for analysis in this article, for which reliable prior treatment and reliable assessment of primary or secondary glioblastoma status were available. Thirty-eight are clinical primary glioblastomas and 5 are clinical secondary glioblastomas. Additional subsets of glioblastomas were selected to address the question of genetic differences between clinically defined subgroups presented here. As secondary glioblastomas are clearly defined, we primarily sought to expand this group. Thus, an additional set of U133A experiments on clinical grade IV glioblastomas included an additional nine clinical secondary glioblastomas and eight primary glioblastomas. For the comparisons with lower grades done here, nine grade III tumors were included from the Freije et al. study (11). An additional 4 grade II tumors are included here as well as 10 normal brain autopsy samples.

**Microarray procedures and data analysis.** Total RNA was isolated from tumor samples using a TRIzol reagent (Invitrogen Life Technologies, Carlsbad, CA) and was followed by a cleanup on a RNeasy column (Qiagen, Hilden, Germany). cDNA was generated and cRNA probes were generated using standard protocols (12). Aliquots of each sample were hybridized to U133A oligonucleotide microarray (GeneChip Human Genome U133A, Affymetrix, Santa Clara, CA), which represents  $\sim 14,500$  human transcripts. The chips were scanned using the GeneArray scanner (Affymetrix). The CEL files generated by the Affymetrix Microarray Suite (MAS 5.0) were converted into DCP files using the DNA-Chip Analyzer (dChip 1.3, <http://biosun1.harvard.edu/complab/dchip/>). The DCP files were globally normalized, and gene expression values were generated using the dChip implementation of perfect match minus mismatch model-based expression index. All group comparisons were done in dChip.

**Gene annotation and tissue expression distribution.** Functional annotation of genes was obtained from published literature (PubMed) and the GeneReport of the Source database (<http://source.stanford.edu>). The data for normalized expression distribution for tissue type were obtained from UCLA normal tissue transcription database (<http://www.dev.gmod.org/>) established in our laboratory, which unified data from OMIM, SwissProt, LocusLink, Unigene, Genbank, and Gene Card.

**Real-time quantitative and semiquantitative RT-PCR.** To verify the microarray data, real-time quantitative RT-PCR was carried out with MJ Opticon PCR Analyzer (MJ Research, Inc., Waltham, MA) using SYBR Green PCR Core Reagents (Applied Biosystems, Foster City, CA). All RNA samples extracted from glioblastoma biopsies were digested with DNase I, which is free of RNase, before reverse transcription (Ambion, Inc., Austin, TX). Total RNA (2  $\mu\text{g}$ ) was used as a template for RT-PCR. cDNA synthesis was done for one cycle at  $50^{\circ}\text{C}$  for 30 minutes and  $94^{\circ}\text{C}$  for 2 minutes. The PCR reactions were cycled 30 times [ $50^{\circ}\text{C}$  for 2 minutes,  $95^{\circ}\text{C}$  for 10 minutes ( $94^{\circ}\text{C}$  for 15 seconds,  $58-61^{\circ}\text{C}$  for 1 minute,  $72^{\circ}\text{C}$  for 1 minute)  $\times$  30 cycles], and the fluorescence was measured at the end of each cycle to construct amplification curves. The melting curve was determined to verify that the PCR product of appropriate size was created. Quantitation of transcripts was calculated based on a titrated standard curve co-run in the same experiment and calibrated with the expression level of a housekeeping gene ( $\beta$ -actin and glyceraldehyde-3-phosphate dehydrogenase). All determinations were done in duplicate. Primer 3 Input (primer3\_www.cgi v 0.2) was used to select primers and nonredundant specific primer sequences was verified using BLAT Search Genome (<http://genome.ucsc.edu>) and National Center for Biotechnology Information BLAST (<http://www.ncbi.nlm.nih.gov/blast/Blast.cgi>). The primer sequences and expected size of amplified PCR products are listed at Supplementary Table S1. The specificity of selected PCR products was confirmed by sequencing.

**Tissue microarray and immunohistochemistry.** A high-density glioblastoma tissue array was constructed consisting of three representative 0.6-mm cores from formalin-fixed, paraffin-embedded tissue blocks from each of 60 primary glioblastomas, 16 secondary glioblastomas, and 15 normal brain tissues. Sections were stained with polyclonal antibody to YKL-40/cartilage glycoprotein-39 (1:200, Quidel Corp., San Diego, CA) or control antibody for overnight at  $4^{\circ}\text{C}$ . Subsequent immunodetection was done using Vectastain ABC Standard kit (Vector Laboratories, Burlingame, CA) and Vector NovaRED (Vector Laboratories). Staining intensity was scored by a neuropathologist (K.Y.) based on a scale of 0 to 2 in which negatively stained specimens were graded 0, weakly positive samples were graded 1, and strongly positive spots were graded 2 (13). The significance of differences in the incidence of YKL-40/cartilage glycoprotein-39 expression in glioblastoma subgroups and normal brain tissue was calculated using one-tailed, two-proportion  $Z$ -test.

## Results

**Identification of GAGs.** We analyzed the expression of  $\sim 14,500$  well-characterized human genes (22,283 probe sets) using Affymetrix GeneChip U133A for 102 brain tumors and normal brain tissues consisting 46 grade IV primary glioblastomas, 14 secondary glioblastomas, 13 astrocytomas (4 grade II and 9 grade III), 19 oligodendromas (8 grade II and 11 grade III), and 10 normal brain tissues. To identify gain-of-function genes correlated with the malignant features of glioblastomas, we compared the mean level of normalized transcript levels in each of the two clinically defined glioblastoma groups versus the grade II and III astrocytomas. Probe set signals on the U133A array that were  $\geq 2.5$ -fold in each glioblastoma group versus the astrocytoma group and with a pairwise  $t$  test ( $P < 0.05$ ) were selected. In addition, to avoid inclusion of low-level and unreliable signals, the higher signal needed to exceed 100 and be called present by MAS 5.0 in  $>20\%$  of the samples. Genes that were identified using these two filtering criteria were designated as either primary or secondary GAGs. Expression patterns across a set of 16 samples were verified by real-time quantitative RT-PCR analysis of eight selected genes with an average correlation of 0.88 (0.77-0.94).

**Shared GAGs reflect common characteristics of hyperproliferation, hypervascularity, and apoptotic resistance in both glioblastoma subgroups.** When compared with lower-grade astrocytomas under the defined comparison criteria, 36 GAGs were identified from the secondary glioblastoma group comparison and 73 GAGs were identified from the primary glioblastoma group comparison (data not shown). Because secondary glioblastomas cannot be distinguished from primary glioblastomas histopathologically, we anticipated identifying common genes underlying the phenotypic similarity. Indeed, 15 GAGs were identified in both pairwise comparisons (Fig. 1A; Table 1). These 15 genes share some functional categorization and are involved in mitosis and extracellular response-associated genes. However, although commonly overexpressed in both types of glioblastomas, there were quantitative differences in expression levels between secondary glioblastomas and primary glioblastomas. The secondary glioblastomas showed higher expression in several mitotic cell cycle-associated genes (*RRMP*, *TYMS*, *TOP2A*, *CENPF*, *HEC*, *CDC2*, *TOPK*, and *ANKT*), whereas primary glioblastomas exhibited higher expression of several extracellular response-associated genes (*ADM*, *VEGF*, *FCGBP*, and *COL4A1/COL4A2*). The most highly expressed gene in the secondary glioblastoma subgroup relative to the lower-grade tumors was hepatocyte growth factor receptor (*MET*), which was also induced in the primary glioblastomas but to a lesser degree. Conversely, the most overexpressed gene in the

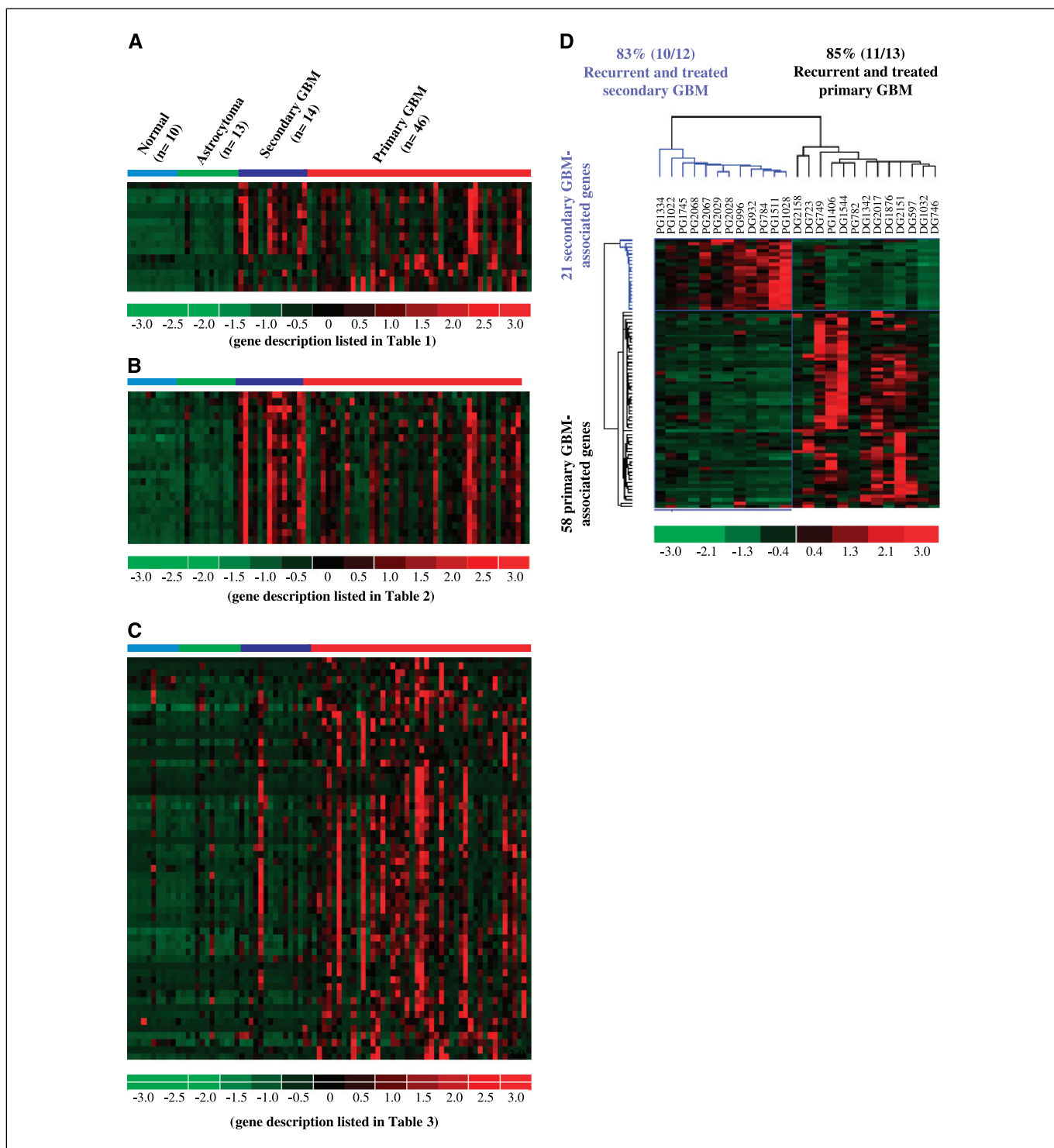


**Figure 1.** GAGs overexpressed in glioblastomas relative to lower-grade gliomas. All plots show normalized gene expression values converted into a heat map. The  $\log_2$  of the fold difference is indicated by the heat map scale at the *bottom*. Each column is an individual tissue or tumor sample organized into histologic groups defined at the *top*. Each row is a single probe set measurement of transcript abundance for an individual gene. The genes are listed in the same order from *top* to *bottom* as the corresponding tables for each of the four lists. All genes were filtered to select transcripts with  $\geq 2.5$ -fold expression in the respective glioblastoma (GBM) group relative lower-grade astrocytomas ( $P < 0.05$ ,  $t$  test). *A*, shared GAGs overexpressed in glioblastomas: 15 shared GAGs were identified from the intersection of the comparisons of primary glioblastomas versus lower-grade astrocytomas and secondary glioblastomas versus lower-grade astrocytomas. *B*, GAGs overexpressed uniquely in secondary glioblastomas: 21 secondary GAGs were defined as being uniquely detected with a  $>2.5$ -fold overexpression in the secondary glioblastoma group compared with the lower-grade astrocytomas and not overexpressed within the primary glioblastoma group using the same criteria. *C*, GAGs overexpressed uniquely in primary glioblastomas: 58 primary GAGs were defined as overexpressed 2.5-fold relative to lower-grade astrocytomas and not detected in the secondary glioblastomas comparison using the same criteria. *D*, unsupervised sample clustering of primary and secondary glioblastomas that are recurrent and had treatment using 21 secondary glioblastomas (Table 2) and 58 primary GAGs (Table 3).

**Table 1.** Shared GAGs expressed at higher levels in both primary and secondary glioblastomas compared with astrocytomas

Gene	Symbol	Accession no.	Chromosome	Secondary glioblastomas		Primary glioblastomas	
				Fold	<i>P</i>	Fold	<i>P</i>
<i>Met proto-oncogene</i>	<i>MET</i>	BG170541	7q31	8.48	0.017936	4.21	0.045314
<i>Ribonucleotide reductase M2 polypeptide</i>	<i>RRMP</i>	NM_001034.1	2p25	3.46	0.00015	3.52	0
<i>Thymidylate synthetase</i>	<i>TYMS</i>	NM_001071.1	18p11	2.77	0.00084	2.5	0.000025
<i>Topoisomerase (DNA) II<math>\alpha</math>, 170 kDa</i>	<i>TOP2A</i>	NM_001067.1	17q21	4.24	0.006921	2.65	0.001064
<i>Centromere protein F, 350/400 kDa</i>	<i>CENPF</i>	NM_005196.1	1q32	6.41	0.001846	2.98	0.000407
<i>Highly expressed in cancer</i>	<i>HEC</i>	NM_006101.1	18p11	3.57	0.003301	2.83	0
<i>Cell division cycle 2, G<sub>1</sub>-S and G<sub>2</sub>-M</i>	<i>CDC2</i>	AL524035	10q21	4	0.008511	2.5	0.000008
<i>Hypothetical protein</i>	<i>FLJ23468</i>	NM_024629.1	4q35	3.63	0.00146	2.5	0.000023
<i>T-LAK cell-originated protein kinase</i>	<i>TOPK</i>	NM_018492.1	8p21	3.64	0.009279	2.68	0.00019
<i>Nucleolar protein ANKT</i>	<i>ANKT</i>	NM_016359.1	15q14	3.44	0.000624	2.56	0.000004
<i>Adrenomedullin</i>	<i>ADM</i>	NM_001124.1	11p15	3.39	0.020445	6.76	0.00003
<i>Vascular endothelial growth factor</i>	<i>VEGF</i>	M27281.1	6p12	3.12	0.004844	6.1	0.000001
<i>Fc fragment of IgG-binding protein I</i>	<i>FCGBP</i>	NM_003890.1	19q13	2.63	0.036568	3.5	0.000005
<i>Collagen type IV, <math>\alpha</math>1</i>	<i>COL4A1</i>	NM_001845.1	13q34	3	0.002538	3.6	0.000003
<i>Collagen type IV, <math>\alpha</math>2</i>	<i>COL4A2</i>	AK025912.1	13q34	2.65	0.005812	3.2	0.000003

NOTE: Analysis was based on a cutoff of a 2.5-fold increase in relative expression ( $P < 0.05$ ) in glioblastomas compared with astrocytomas.

primary glioblastomas compared with the lower-grade tumors was *ADM*, which was induced in the secondary tumors but to a lesser degree. Both of these genes are well-characterized tumor survival factors, which have been shown to play a critical role in cancer cell division, antiapoptosis, cell migration, and tumor neovascularization (14, 15). Activation of the receptor tyrosine kinase Met promotes cell survival by activating phosphatidylinositol 3-kinase signaling cascade (16). Additionally, Met sequesters Fas, circumventing programmed cell death (17). *ADM*, which is up-regulated during hypoxic insult, promotes the growth and migration of endothelial cells (18), and has also been implicated as a potential immune suppressor substance (15). The detection of up-regulated VEGF transcripts likely reflects the hypoxia, which promotes an angiogenic response (19).

**Distinct GAGs identified in secondary glioblastomas reflect aggressive cell cycle.** Twenty-one distinct GAGs were overexpressed only in the secondary glioblastomas. Remarkably, all 21 genes are associated with mitotic cell cycle (Fig. 1B; Table 2). More specifically, these genes are involved in control of cell cycle (*CKS2*, *CDKN3*, *GAS1*, *CCNBI*, *UBE2C*, and *FOXM1*), DNA synthesis and repair (*ECT2* and *PIR51*), cytokinesis and movements of spindle and chromosomes (*RAMP*, *PRC1*, *TMSNB*, *KIF2A*, *KIF14*, and *KIF20A*), DNA bending (*HMGB2*), kinetochore function (*ZWINT*), chromatid separation and regulation of TP53 (*PTTG1*), and mitotic chromosome condensation (*HCAP-G*). Among these genes, *FOXMI*, which is a transcription factor that regulates the expression of transcription network of genes that are essential for DNA replication and mitosis, showed the highest fold increase (20). We then viewed the gene expression distribution among various types of tissue for these 21 genes using our human tissue transcription database (<http://www.dev.gmod.org/>). The results indicated that most transcripts (19 of 21) were highly expressed in proliferative tissues, fetal livers, and testis (germ cells; see Supplementary Fig. S1), which are indicative of the genes known expression in mitotically active cells. A similar set of overexpressed genes were identified when comparative analyses were done

between secondary glioblastomas and the group of oligodendromas (grade II and III; data not shown).

**Distinct GAGs identified in primary glioblastomas reflect a tumor cell stromal response.** Fifty-eight GAGs that are overexpressed only in primary glioblastomas when compared with astrocytomas reflect the processes of the host-tumor interaction that promote the well-recognized invasive phenotype of glioblastomas (Fig. 1C; Table 3). The annotation of the selected genes reflects the *in situ* stromal response of the cancer cells. The list includes genes that are associated with inflammation, coagulation, immune/complement responses (*SERPINA1/SERPINA3*, *SERPINE1*, *PTX3*, *C5RI*, *FCGR3B*, *CEBPD*, and *TIMPI*), angiogenesis (*IL-8*, *CAI*, and *CA2*), extracellular matrix (ECM) remodeling (*COL5A1*, *COL6A2*, *MMP-9*, and *CIR*), and status of hypoxia/angiogenesis (*HIP-2*). Moreover, genes that may function as anti-oxidants or promoters for antiapoptotic activities (*CAIII*, *SOD2*, *DPYD*, *NNMT*, and *UPP1*) were identified and are potential predictors for the chemoradiation-resistant phenotypes. The presence of two transforming growth factor- $\beta$  (TGF- $\beta$ ) target genes (*TGFBI* and *TAGLN*) suggested that TGF- $\beta$  signaling is involved in malignant progression, whereas two stress-responsive genes (*HO* and *SLC16A3*) reflect inflammatory insults and perhaps a glycolysis shift. The overexpression of monocyte chemotactic factor (*CCL*) corresponded to a group of genes reflected influx of tumor-associated macrophage (*CD14*, *CD163*, *STAB1*, *Z391G*, *LYZ*, and *IFI30*), indicating a more pronounced inflammatory component of primary glioblastomas relative to secondary glioblastomas.

A series of genes that are highly expressed in mesenchymal tissues but not neural or glial cells were identified. These include genes that are typically expressed in tissues like bone, cartilage, tendon, ligament, fat, and muscle (*CHI3L1*, *CHI3L2*, *GPNMB*, *LOX*, *TIA-2*, *COLV/VI*, *BGN*, *MEOX2*, *CAIII*, and *TAGLN*). In particular, *CAIII* and *MEOX2* exceed a 10-fold increase when compared with astrocytomas. *CAIII* functions as an oxygen radical scavenger and hence protects cells from oxidative stress (21), whereas *MEOX2* has a role in mesoderm induction and is an important regulator of vertebrate

limb myogenesis (22). Notably, 11 primary GAGs are located at chromosome 7 (*MET*/7q31, *HIF-2*/7q32, *CAV1*/7q31, *CAV2*/7q31, *SERPINE1*/7q21, *PBEF*/7q22, *GPNMB*/7p15, *UPP1*/7, *MEOX2*/7p22, *EGFR*/7p12, and *SEC61G*/7p11; Tables 1 and 3; ref. 23) and 8 of them were reported to be associated with Akt phosphorylation, anti-apoptosis, hypoxia, angiogenesis, and coagulation, which corresponds to the reported amplification of chromosome 7 in primary glioblastomas (24–28). Detection of increased *IGFBP2* transcripts verified previous reports (29). Analysis of the human tissue transcription database confirmed the preferential expression of these GAGs in multiple stromal/mesenchymal tissue types, including cartilage, cultured chondrocytes, muscle, endothelium (aorta), bone marrow, and monocytes/macrophage (see Supplementary Fig. S3). Similarly, comparable transcription profiles of GAGs were obtained when comparative analysis was done against the group of oligodendromas, which showed a dominant group of overexpressed genes that are associated with mesenchymal cells (data not shown).

**Does prior treatment of secondary glioblastomas account for the differences between secondary and primary glioblastomas?** To rule out the possibility that the distinct glioblastoma progression-associated genes identified between two subgroups are due to selection pressure (e.g., radiation or chemotherapy), we conducted clustering based analysis of a set of primary glioblastoma ( $n = 13$ ) and secondary glioblastoma ( $n = 12$ ) samples that were recurrent and had been treated before tumor sampling in two different ways. The 25 tumor specimens meeting criteria above were hierarchically clustered using normalized data for all 79 defined type-specific GAGs (21 secondary GAGs and 58 primary GAGs). The predominant subdivision in the tumors is on the basis of primary versus secondary definition: 85% (11 of 13) of the treated primary glioblastomas were clustered by overexpression of

virtually all 58 primary GAGs, whereas 83% (10 of 12) of the treated secondary glioblastomas were clustered by overexpression of 21 secondary GAGs (Fig. 1D). These analyses were restricted to the already defined primary and secondary GAGs and indicate that both tumor groups, regardless of prior treatment, cluster within their clinical grouping based on gene expression of the selected GAGs. Thus, prior treatment is not disrupting this identified gene expression signature of primary and secondary glioblastomas nor is it driving the selection of the genes.

**Differential expression of cartilage glycoprotein-39 (*CHI3L1*) in glioblastoma subgroups.** Based on our analysis, we consistently observed a significant up-regulation of *CHI3L1* gene expression in primary glioblastomas when compared with low-grade astrocytomas or secondary glioblastomas. To verify this finding, a tissue microarray consisting of tumor cores and matching normal brain counterparts from 60 primary glioblastomas and 16 secondary glioblastomas was constructed and immunohistochemically stained using commercially available antibody to cartilage glycoprotein-39 (YKL-40). *CHI3L1* expression was significantly more frequently detected in the clinically defined primary glioblastoma samples compared with secondary glioblastomas and normal brain. Forty-two percent (25 of 60) of the primary glioblastomas stained positively with average intensities of  $1.7 \pm 0.46$ , whereas 12.5% (2 of 16;  $P = 0.0152$ ) and 6.7% (1 of 15;  $P = 0.0054$ ) were positively stained in secondary glioblastomas and normal brain, respectively. All three positive stains in secondary glioblastomas and a normal brain specimen were weak (Fig. 2).

**Discussion**

In this study, we used a large-scale gene expression analysis to further characterize clinical subgroups of glioblastomas. We aimed

**Table 2.** Distinct GAGs expressed at higher levels in secondary glioblastomas compared with astrocytomas

Gene	Symbol	Accession	Chromosome	Fold change	P
<i>Homo sapiens mRNA; cDNA DKFZp564F112</i>		AL049987.1		2.51	0.000299
<i>Growth arrest-specific 1</i>	<i>GAS1</i>	NM_002048.1	9q21	2.58	0.004934
<i>RAD51-interacting protein</i>	<i>PIR51</i>	BE966146	12p13	2.81	0.000739
<i>Thymosin β, identified in neuroblastoma cells</i>	<i>TMSNB</i>	NM_021992.1	Xq21	3.26	0.000834
<i>KLAA0101 gene product</i>		NM_014736.1	15q22	2.62	0.000563
<i>Cyclin-dependent kinase inhibitor 3</i>	<i>CDKN3</i>	AF213033.1	14q22	2.53	0.004978
<i>High-mobility group box 2</i>	<i>HMGB2</i>	BC000903.1	4q31	2.75	0.000438
<i>Ubiquitin-conjugating enzyme E2C</i>	<i>UBE2C</i>	NM_007019.1	20q13	2.92	0.000382
<i>Retinoic acid-regulated nuclear matrix-associated protein</i>	<i>RAMP</i>	NM_016448.1	1	2.94	0.014477
<i>CDC28 protein kinase regulatory subunit 2</i>	<i>CKS2</i>	NM_001827.1	9q22	3.08	0.00485
<i>Epithelial cell transforming sequence 2 oncogene</i>	<i>ECT2</i>	NM_018098.1	3q25	2.97	0.001624
<i>Kinesin family member 20A</i>	<i>KIF20A</i>	NM_005733.1	5q31	3.24	0.000546
<i>Cyclin B1</i>	<i>CCNB1</i>	BE407516	5q12	2.48	0.00095
<i>Pituitary tumor-transforming 1</i>	<i>PTTG1</i>	NM_004219.2	5q35	2.8	0.000862
<i>Chromosome condensation protein G</i>	<i>HCAP-G</i>	NM_022346.1	4p16	3.37	0.003616
<i>ZW10 interactor</i>	<i>ZWINT</i>	NM_007057.1	10q21	2.68	0.006086
<i>asp (abnormal spindle)-like</i>	<i>ASPM</i>	NM_018123.1	1q31	3.24	0.003574
<i>Protein regulator of cytokinesis 1</i>	<i>PRC1</i>	NM_003981.1	15q26	3.45	0.0026
<i>Kinesin family member 14</i>	<i>KIF14</i>	NM_014875.1	1pter-q31.3	2.5	0.006231
<i>Forkhead box M1</i>	<i>FOXM1</i>	NM_021953.1	12p13	3.8	0.000976
<i>Kinesin family member 4A</i>	<i>KIF4A</i>	NM_012310.2	Xq13	2.83	0.00078

NOTE: Analysis was based on a cutoff of a 2.5-fold increase in relative expression ( $P < 0.05$ ) in secondary glioblastomas compared with astrocytomas.

**Table 3.** Distinct GAGs expressed at higher levels in primary glioblastomas compared with astrocytomas

Gene	Symbol	Accession	Chromosome	Fold change	P
<i>Carbonic anhydrase III, muscle specific</i>	<i>CAIII</i>	NM_005181.2	9q13	11.46	0.007594
<i>Lactotransferrin</i>	<i>LTF</i>	NM_002343.1	3q21	3.8	0.00565
<i>Human clone 137308 mRNA, partial cds.</i>		AU134977		3.02	0.005225
<i>Solute carrier family 2 (facilitated glucose transporter), member 3</i>	<i>SLC2</i>	NM_006931.1	12p13	2.65	0.000054
<i>Hypoxia-inducible protein 2</i>	<i>HIF-2</i>	NM_013332.1	7q32	2.56	0.001092
<i>Guanylate-binding protein 1, IFN-inducible, 67 kDa</i>	<i>GBP1</i>	NM_002053.1	1p22	2.71	0.000028
<i>Chitinase 3-like 2</i>	<i>CHI3L2</i>	U58515.1	1p13	2.68	0.000827
<i>Proteinase inhibitor, clade A (antitrypsin), member 3</i>	<i>SERPINA3</i>	NM_001085.2	14q32	2.64	0.000716
<i>Heat shock 70-kDa protein 6</i>	<i>HSP70B</i>	NM_002155.1	1	3.75	0.000047
<i>Caveolin 2</i>	<i>CV2</i>	NM_001233.1	7q31	2.46	0.000043
<i>Heme oxygenase (decycling) 1</i>	<i>HO</i>	NM_002133.1	22q13	3.2	0.000088
<i>Matrix metalloproteinase-9 (92-kDa type IV collagenase)</i>	<i>MMP-9</i>	NM_004994.1	20q11	4.38	0.002731
<i>Biglycan</i>	<i>BGN</i>	AA845258	Xq28	2.78	0.000053
<i>Collagen type VI, <math>\alpha</math>2</i>	<i>COL6A2</i>	AY029208.1	21q22	2.93	0.019421
<i>Collagen type V, <math>\alpha</math>1</i>	<i>COL5A1</i>	AI983428	9q34	2.46	0.03049
<i>Fc fragment of IgG, low-affinity IIIb, receptor for (CD16)</i>	<i>FCGR3B</i>	NM_000570.1	1q23	2.61	0.000285
<i>Chromosome 8 open reading frame 4</i>	<i>C8orf4</i>	NM_020130.1	8p11	4.05	0.000735
<i>Chemokine (C-C motif) ligand 2</i>	<i>CCL</i>	S69738.1	17q11	2.66	0.002211
<i>Interleukin-8</i>	<i>IL-8</i>	NM_000584.1	4q13	4.83	0.00097
<i>Interleukin-8 COOH-terminal variant (IL8) mRNA, complete cds.</i>		AF043337.1		3	0.01931
<i>Superoxide dismutase 2, mitochondrial</i>	<i>SOD2</i>	W46388	6q25	3.23	0
<i>H. sapiens, clone IMAGE:4711494, mRNA</i>		BF575213		2.53	0
<i>Pre-B-cell colony-enhancing factor</i>	<i>PBEF</i>	NM_005746.1	7q22	3.76	0.000003
<i>Complement component 1, r subcomponent</i>	<i>C1R</i>	AL573058	12p13	3.13	0.000044
<i>CCAAT/enhancer-binding protein, <math>\delta</math></i>	<i>CEBPD</i>	AV655640	8p11	2.54	0.00003
<i>Proteinase inhibitor, clade A (antitrypsin), member 1</i>	<i>SERPINA1</i>	NM_000295.1	14q32	2.62	0.000155
<i>Nicotinamide N-methyltransferase</i>	<i>NNMT</i>	NM_006169.1	11q23	8.71	0.000155
<i>Glycoprotein (transmembrane) nmb</i>	<i>GNPMB</i>	NM_002510.1	7p15	2.71	0.002098
<i>Dihydropyrimidine dehydrogenase</i>	<i>DPYD</i>	NM_000110.2	1p22	2.94	0.000015
<i>Complement component 5 receptor 1 (C5a ligand)</i>	<i>C5R1</i>	NM_001736.1	19q13	3.57	0.000125
<i>S100 calcium-binding protein A8 (calgranulin A)</i>	<i>S100A8</i>	NM_002964.2	1q21	3.84	0.000366
<i>Lysozyme (renal amyloidosis)</i>	<i>LYZ</i>	AV711904	12q14	2.5	0.0012694
<i>IFN-<math>\gamma</math>-inducible protein 30</i>	<i>IFI30</i>	NM_006332.1	19p13	3.09	0.00002
<i>CD14 antigen</i>	<i>CD14</i>	NM_000591.1	5q31	2.66	0.000031
<i>Ig superfamily protein</i>	<i>Z391G</i>	NM_007268.1	Xq12	2.61	0.000006
<i>CD163 antigen</i>	<i>CD163</i>	NM_004244.1	12p13	3.86	0.000011
<i>Stabilin 1</i>	<i>STAB1</i>	NM_015136.1	3p21	2.63	0.000073
<i>Solute carrier family 16 (monocarboxylic acid transporters)</i>	<i>SLC16A3</i>	NM_004207.1	17q25	3.27	0.000001
<i>Transforming growth factor-<math>\beta</math> induced, 68 kDa</i>	<i>TGVB1</i>	NM_000358.1	5q31	2.71	0.00091
<i>Fibronectin 1</i>	<i>FNI</i>	BC005858.1	2q34	2.52	0.000002
<i>Epithelial membrane protein 3 S100 calcium-binding protein A11 (Calgizzarin)</i>	<i>EMP3</i>	NM_001425.1	19q13	2.73	0.000175
	<i>S100A11</i>	NM_005620.1	1q21	2.64	0.00007
<i>Tissue inhibitor of metalloproteinase 1 (collagenase inhibitor)</i>	<i>TIMP1</i>	NM_003254.1	Xp11	2.58	0.002723
<i>Caveolin 1, caveolae protein, 22 kDa</i>	<i>CAVI</i>	AU147399	7q31	3.01	0.000025
<i>Lysyl oxidase</i>	<i>LOX</i>	L16895	5q23	5.85	0.000442
<i>Proteinase inhibitor, clade E (plasminogen activator inhibitor type 1)</i>	<i>SERPINE1</i>	NM_000602.1	7q21	3.15	0.001055
<i>Transgelin</i>	<i>TAGLN</i>	NM_003186.2	11q23	3.57	0.000112
<i>Thrombospondin 1</i>	<i>THBS1</i>	NM_003246.1	5q15	3.18	0.015815
<i>Uridine phosphorylase</i>	<i>UPP1</i>	NM_003364.1	7	2.53	0.000003
<i>Chitinase 3-like 1 (cartilage glycoprotein-39)</i>	<i>CHI3L1</i>	M80927.1	1q32	4.17	0.000726
<i>Pentaxin-related gene, rapidly induced by interleukin-1<math>\beta</math></i>	<i>PTX3</i>	NM_002852.1	3q25	5.55	0.000292
<i>Lung type 1 cell membrane-associated glycoprotein</i>	<i>TIA-2</i>	BF337209	1p36	3.07	0.000054
<i>Short stature homeobox 2</i>	<i>SHOX2</i>	AF022654.1	3q25	2.59	0.000151
<i>Mesenchyme homeobox 2 (growth arrest-specific homeobox)</i>	<i>MEOX2</i>	NM_005924.1	7p22	10.31	0.000219
<i>Insulin-like growth factor-binding protein 2, 36 kDa</i>	<i>IGFBP2</i>	NM_000597.1	2q33	2.49	0.007258
<i>Fatty acid-binding protein 5 (psoriasis-associated)</i>	<i>FABP5</i>	NM_001444.1	8q21	2.86	0.00001
<i>Epidermal growth factor receptor</i>	<i>EGFR</i>	NM_005228.1	7p12	2.66	0.003366
<i>Sec61<math>\gamma</math></i>	<i>SEC61G</i>	NM_014302.1	7p11	2.49	0.000013

NOTE: Analysis was based on a cutoff of a 2.5-fold increase in relative expression ( $P < 0.05$ ) in primary glioblastomas compared with astrocytomas.

to elucidate molecular pathway correlates of observed clinical features of primary and secondary glioblastomas that distinguish them from lower-grade astrocytomas. Our analytic strategy extracted lists of genes that are expressed in glioblastomas but not the lower-grade tumors or normal brain tissue. The comparison to lower-grade astrocytomas was done to attempt to select for genes, which are specific to the end malignant transformation into the highly invasive glioblastomas. The described short lists of genes are descriptive and partially explanatory of known tumor behavior, pathology, and resistance to therapy and provide an insight into how the deregulation of multigene networks leads to tumor malignancy. Moreover, the GAGs identified that are uniquely expressed in primary and secondary glioblastomas provide new leads into diverse mechanisms and properties underlying distinct transformation events or perhaps distinct cells of origin of glioblastoma subgroups. These data extend and complement recent studies using two-dimensional gel analysis, which indicated that clinical and genetic differences in primary and secondary glioblastomas could be recognized at the protein level (30).

In our study, we used a clinical definition of secondary designation restricted to those tumors with clear prior evidence of a lower-grade tumor. In contrast, the clinical definition of primary glioblastomas is more tenuously based on lack of previous evidence of lower-grade tumor. One would expect that at least a subset of clinically defined primary glioblastomas had a lower-grade initial lesion that progressed asymptotically and would biologically resemble the secondary glioblastoma group. Indeed, there is a strong trend toward the clinical secondary glioblastomas having similar coexpression of secondary GAGs (10 of 14), whereas 24 of 45 of the clinical primary glioblastomas have a similar overexpression of the primary GAGs and instead have a pattern of expression more similar to the overall secondary glioblastoma group. Thus, our data suggest that as many as half of clinically defined primary glioblastomas have the genetic signature of secondary glioblastomas and thus may develop from

lower-grade tumors *in vivo* that are clinically unrecognized. However, this group of primary glioblastomas, which group with the secondary tumors, occur in individuals at a mean age (51 years) range that is typical of primary glioblastomas with the primary glioblastoma signature (54 years) as opposed to the clinically defined secondary glioblastomas (39 years).

Some differences in the frequency of distinct genetic alterations in primary and secondary glioblastomas have been well described (31). These known genomic alterations may partly explain our detection of differential transcription profiles in glioblastoma subgroups. For instance, the large number of genes on chromosome 7, which are up-regulated in primary glioblastomas, may be indicative of chromosome 7 amplification. Further, our data support the notion that mutation or dysfunction of prominent cell cycle regulators is a major mechanism for the malignant transformation in secondary glioblastomas. Deletion of chromosome 17 and/or mutation in p53 have been reported in ~60% of secondary glioblastomas but <10% of primary glioblastomas (32). The p53 tumor suppressor is highly interconnected and mutation of p53 severely disrupts normal cell cycle progression through the modulation of genes that mediate the arrest of cells in the G<sub>1</sub> or G<sub>2</sub> phase (33, 34). p53 mutations, however, are usually found in the low-grade lesions of astrocytomas, indicating that p53 alteration is an early event in astrocytoma progression. A recent report further suggests that retinoblastoma tumor susceptibility gene (*Rb*) may function in the maintenance of chromosome stability by influencing mitotic progression, faithful chromosome segregation, and structural remodeling of mitotic chromosomes (35). LOH in the region containing the *Rb* gene is found in high-grade astrocytomas but not in low-grade astrocytomas, suggesting that disruption of *Rb* is important for the continued malignant transformation to glioblastomas (36).

Primary GAGs strongly reflected a desmoplastic-like phenotype with deposition of abundant collagen. Several markers that implicated the influx of tumor-associated macrophages and lymphocytes were identified. This observation implicates that

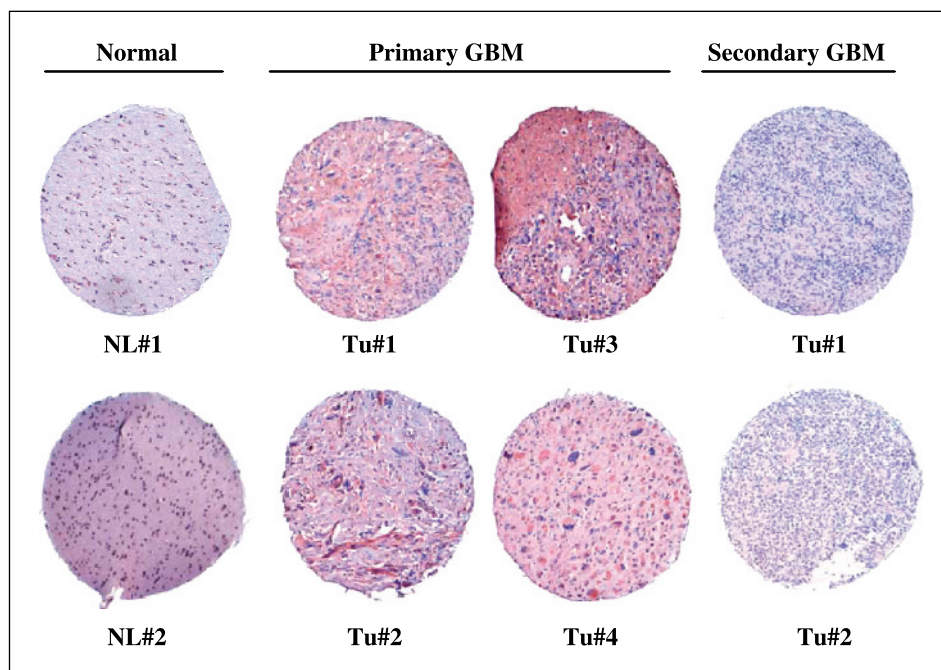


**Figure 2.** Expression of cartilage glycoprotein-39 (YKL-40) in glioblastoma subgroups. Representative immunohistochemical stainings of YKL-40 in clinical glioblastoma subgroups and normal brain. A subset of the images from a tissue array are shown. Each core is 0.06 mm across. Strong positivity of YKL-40 antibody staining was detected in four primary glioblastomas; negative/weak staining was detected in two secondary glioblastomas and two normal brain cores shown.

stromal cells likely participate in promoting such a wound-like phenotype in glioblastoma tumor *in situ*. This link between gene expression signature of fibroblast serum response and cancer progression has been reported (37). Degradation of the ECM by matrix metalloproteinase (MMP) is required in endothelial cell migration, organization, and angiogenesis. *THBS1* promotes tumor invasion of collagens by enhanced MMP-9 production (38) and *IL-8* promotes inflammation, complement response, and coagulation (39). Tumor progression is commonly associated with dysregulation of thrombotic and fibrinolytic processes. The up-regulation of transcripts of inhibitors for proteinase, plasmin, and MMP (*SERPINA1*, *SERPINA3*, *PAI-1*, and *TIMP1*) may function to sustain thrombus formation and prevent fibrinolysis, subsequently inducing coagulative necrosis and hypoxia within pseudopalisades (31, 40). Subsequently, hypoxia induces angiogenesis (*HIF-2*, *MET*, *ADM*, *VEGF*, and *IL-8*) and pseudopalisading cell migration that escape from necrotic zone, thus favoring tumor outgrowth (40).

It seems that the molecular distinction between primary and secondary glioblastomas is not due to a higher frequency of prior treatment in the secondary glioblastoma group but rather reflect genetic differences between the two mechanisms for glioblastoma oncogenesis, which are maintained within the tumors. This conclusion was supported by the comparison of the two glioblastoma subgroups that are both recurrent and had treatment before the biopsy. In addition, in our study, patients with secondary glioblastomas have average younger age ( $37 \pm 9$  years) than the patients with primary glioblastomas ( $51 \pm 15$  years). We previously published results that included some of the clinical primary glioblastoma samples presented in the analyses presented here. Although most of those samples were clinically primary glioblastomas, there was strong heterogeneity within the glioblastomas. In our previous expression study, which included 63 glioblastomas (11), most glioblastoma samples grouped within two hierarchical clusters; one cluster is defined by overexpression of genes involved in mitosis (HC2A) and the other one is defined by overexpression of ECM components and regulators (HC2B). Thus, the previously defined HC2B group with ECM overexpression is greatly enriched in primary glioblastomas.

In summary, our study explored a complexity of molecular pathways and networks that drives the survival, progression, and invasion of glioblastomas. Several key genes on the list of GAGs corresponded well to previous reports (11, 13, 29, 41–43). Moreover, these data support the concept that the interplay between glioblastoma-derived bone/cartilage-associated factors and tumor-associated stromal cells (fibroblasts, endothelium, and inflammatory cells) plays a key role in the malignant aggressiveness of primary glioblastomas. It has been reported that osteopontin, osteoactivin (*GPNUMB*), and osteonectin stimulate tumor invasion and secretion of urokinase-type plasminogen activator through the activation of EGFR, Met, and Akt signaling pathways (44–47). Additional immunostainings of tissue arrays (osteonectin and tenascin C; data not shown) further confirm the mesenchymal properties in primary glioblastomas. Based on our previous study (11) and current observation of a distinct set of genes being expressed in glioblastomas are associated with mesenchymal cells, we have pursued the analysis of primary glioblastoma-derived cell cultures and have indicated that these tumor cell explants possess stem-like properties and can be differentiated into multiple mesenchymal cell lineages,<sup>7</sup> further highlighting profound differences in glioblastoma subtype and opening up the question regarding the cellular origin of a subset of glioblastomas.

## Acknowledgments

Received 1/12/2005; revised 8/15/2005; accepted 9/28/2005.

**Grant support:** National Cancer Institute grant U01CA88173, Accelerate Brain Cancer Cure, Henry Singleton Brain Tumor Program, Art of the Brain, UCLA DNA Microarray Facility, National Institute of Neurological Diseases and Stroke, National Institute of Mental Health Microarray Consortium grant U24NS43562, Women's Reproductive Health Research Center grant 5K12HD001281 (W.A. Freije), and Integrated Graduate Education and Research Traineeship grant (A. Day).

The costs of publication of this article were defrayed in part by the payment of page charges. This article must therefore be hereby marked *advertisement* in accordance with 18 U.S.C. Section 1734 solely to indicate this fact.

We thank the patients who participated in this study.

<sup>7</sup> Tso et al., unpublished data.

## References

- Shackney SE, Shankey TV. Common patterns of genetic evolution in human solid tumors [review]. *Cytometry* 1997;29:1–27.
- Cai WW, Mao JH, Chow CW, et al. Genome-wide detection of chromosomal imbalances in tumors using BAC microarrays. *Nat Biotechnol* 2002;20:393–6.
- Zhang LH, Qin LX, Ma ZC, et al. Allelic imbalance regions on chromosomes 8p, 17p and 19p related to metastasis of hepatocellular carcinoma: comparison between matched primary and metastatic lesions in 22 patients by genome-wide microsatellite analysis. *Cancer Res Clin Oncol* 2003;129:279–86.
- Smith CA, Pollice AA, Gu LP, et al. Correlations among p53, Her-2/neu, and ras overexpression and aneuploidy by multiparameter flow cytometry in human breast cancer: evidence for a common phenotypic evolutionary pattern in infiltrating ductal carcinomas. *Clin Cancer Res* 2000;6:112–26.
- Morales CP, Souza RF, Spechler SJ. The hallmarks of cancer. *Cell* 2000;100:57–70.
- Scott JN, Revcastle NB, Brasher PM, et al. Long-term glioblastoma multiforme survivors: a population-based study. *Can J Neurol Sci* 1998;25:197–201.
- Prat DJ, Van Meir EG. Vaso-occlusive and prothrombotic mechanisms associated with tumor hypoxia, necrosis, and accelerated growth in glioblastoma [review]. *Lab Invest* 2004;84:397–405.
- Kleihues P, Ohgaki H. Primary and secondary glioblastomas: from concept to clinical diagnosis [review]. *Neuro-oncol* 1999;1:44–51.
- Maruno M, Ninomiya H, Ghulam Muhammad AK, et al. Whole-genome analysis of human astrocytic tumors by comparative genomic hybridization. *Brain Tumor Pathol* 2000;7:21–7.
- Kleihues P, Louis DN, Scheithauer BW, et al. The WHO classification of tumors of the nervous system [review]. *J Neuropathol Exp Neurol* 2002;61:215–25.
- Freije WA, Castro-Vargas FE, Fang Z, et al. Gene expression profiling of gliomas strongly predicts survival. *Cancer Res* 2004;64:6503–10.
- Shai R, Shi T, Kremen TJ, et al. Gene expression profiling identifies molecular subtypes of gliomas. *Oncogene* 2003;22:4918–23.
- Choe G, Horvath S, Cloughesy TF, et al. Analysis of the phosphatidylinositol 3'-kinase signaling pathway in glioblastoma patients *in vivo*. *Cancer Res* 2003;63:2742–6.
- To CT, Tsao MS. The roles of hepatocyte growth factor/scatter factor and met receptor in human cancers [review]. *Oncol Rep* 1998;5:1013–24.
- Cuttitta E, Pio R, Garayoa M, et al. Adrenomedullin functions as an important tumor survival factor in human carcinogenesis [review]. *Microsc Res Tech* 2002;57:110–9.
- Maulik G, Madhiwala P, Brooks S, et al. Activated c-Met signals through PI3K with dramatic effects on cytoskeletal functions in small cell lung cancer. *J Cell Mol Med* 2002;6:539–53.
- Wang X, DeFrances MC, Dai Y, et al. Mechanism of cell survival: sequestration of Fas by the HGF receptor Met. *Mol Cell* 2002;9:411–21.
- Miyashita K, Itoh H, Sawada N, et al. Adrenomedullin provokes endothelial Akt activation and promotes vascular regeneration both *in vitro* and *in vivo*. *FEBS Lett* 2003;544:86–92.
- Terman BI, Stoletoff KV. VEGF and tumor angiogenesis. *Einstein Quart. J Biol Med* 2001;18:59–66.
- Wang X, Kiyokawa H, Denneewitz MB, Costa RH. The Forkhead Box m1b transcription factor is essential for hepatocyte DNA replication and mitosis during mouse liver regeneration. *Proc Natl Acad Sci U S A* 2002;99:16881–6.
- Raisanen SR, Lehenkari P, Tasanen M, et al. Carbonic anhydrase III protects cells from hydrogen peroxide-induced apoptosis. *FASEB J* 1999;13:513–22.
- Mankoo BS, Collins NS, Ashby P, et al. Mox2 is a component of the genetic hierarchy controlling limb muscle development. *Nature* 1999;400:69–73.

23. A, Artan S, Oner U, et al. The importance of genomic copy number changes in the prognosis of glioblastoma multiforme. *Neurosurg Rev* 2004;27:58–64.
24. Li L, Ren CH, Tahir SA, Ren C, Thompson TC. Caveolin-1 maintains activated Akt in prostate cancer cells through scaffolding domain binding site interactions with and inhibition of serine/threonine protein phosphatases PP1 and PP2A. *Mol Cell Biol* 2003;23:9389–404.
25. Feldkamp MM, Lala P, Lau N, Roncari L, Guha A. Expression of activated epidermal growth factor receptors, Ras-guanosine triphosphate, and mitogen-activated protein kinase in human glioblastoma multiforme specimens. *Neurosurgery* 1999;45:1442–53.
26. Xiao GH, Jeffers M, Bellacosa A, et al. Anti-apoptotic signaling by hepatocyte growth factor/Met via the phosphatidylinositol 3-kinase/Akt and mitogen-activated protein kinase pathways. *Proc Natl Acad Sci U S A* 2001;98:247–52.
27. Zhang Q, Wu Y, Chau CH, et al. Crosstalk of hypoxia-mediated signaling pathways in upregulating plasminogen activator inhibitor-1 expression in keloid fibroblasts. *J Cell Physiol* 2004;199:89–97.
28. Hu CJ, Wang LY, Chodosh LA, Keith B, Simon MC. Differential roles of hypoxia-inducible factor 1 $\alpha$  (HIF-1 $\alpha$ ) and HIF-2 $\alpha$  in hypoxic gene regulation. *Mol Cell Biol* 2003;23:9361–74.
29. Sallinen SL, Sallinen PK, Haapasalo HK, et al. Identification of differentially expressed genes in human gliomas by DNA microarray and tissue chip techniques. *Cancer Res* 2000;60:6617–22.
30. Furuta M, Weil RJ, Vortmeyer AO, et al. Protein patterns and proteins that identify subtypes of glioblastoma multiforme. *Oncogene* 2004;23:6806–14.
31. von Deimling A, von Ammon K, Schoenfeld D, et al. Subsets of glioblastoma multiforme defined by molecular genetic analysis. *Brain Pathol* 1993;3:19–26.
32. Watanabe K, Tachibana O, Sata K, et al. Overexpression of the EGF receptor and p53 mutations are mutually exclusive in the evolution of primary and secondary glioblastomas. *Brain Pathol* 1996;6:217–23.
33. Vogelstein B, Lane D, Levine AJ. Surfing the p53 network. *Nature* 2002;408:307–10.
34. Zhao R, Gish K, Murphy M, et al. Analysis of p53-regulated gene expression patterns using oligonucleotide arrays. *Genes Dev* 2003;14:981–93.
35. Zheng L, Lee WH. Retinoblastoma tumor suppressor and genome stability [review]. *Adv Cancer Res* 2002;85:13–50.
36. Henson JW, Schnitker BL, Correa KM, et al. The retinoblastoma gene is involved in malignant progression of astrocytomas. *Ann Neurol* 1994;36:714–21.
37. Chang HY, Sneddon JB, Alizadeh AA, et al. Gene expression signature of fibroblast serum response predicts human cancer progression: similarities between tumors and wounds. *PLoS Biol* 2004;2:E7.
38. Wang TN, Albo D, Tuszynski GP. Fibroblasts promote breast cancer cell invasion by upregulating tumor matrix metalloproteinase-9 production. *Surgery* 2002;132:220–5.
39. Morikawa S, Takabe W, Mataka C, et al. The effect of statins on mRNA levels of genes related to inflammation, coagulation, and vascular constriction in HUVEC. Human umbilical vein endothelial cells. *J Atheroscler Thromb* 2002;9:178–83.
40. Brat DJ, Van Meir EG. Vaso-occlusive and prothrombotic mechanisms associated with tumor hypoxia, necrosis, and accelerated growth in glioblastoma. *Lab Invest* 2004;84:397–405.
41. Tanwar MK, Gilbert MR, Holland EC. Gene expression microarray analysis reveals YKL-40 to be a potential serum marker for malignant character in human glioma. *Cancer Res* 2002;62:4364–8.
42. Rickman DS, Bobek MP, Misek DE, et al. Distinctive molecular profiles of high-grade and low-grade gliomas based on oligonucleotide microarray analysis. *Cancer Res* 2001;61:6885–91.
43. Markert JM, Fuller CM, Gillespie GY, et al. Differential gene expression profiling in human brain tumors. *Physiol Genomics* 2001;5:21–33.
44. Das R, Mahabeshwar GH, Kundu GC. Osteopontin induces AP-1-mediated secretion of urokinase-type plasminogen activator through c-Src-dependent epidermal growth factor receptor transactivation in breast cancer cells. *J Biol Chem* 2004;79:11051–64.
45. Tuck AB, Hota C, Wilson SM, Chambers AF. Osteopontin-induced migration of human mammary epithelial cells involves activation of EGF receptor and multiple signal transduction pathways. *Oncogene* 2003;22:1198–205.
46. Das R, Mahabeshwar GH, Kundu GC. Osteopontin stimulates cell motility and nuclear factor  $\kappa$ B-mediated secretion of urokinase type plasminogen activator through phosphatidylinositol 3-kinase/Akt signaling pathways in breast cancer cells. *J Biol Chem* 2003;278:28593–606.
47. Rich JN, Shi Q, Hjelmeland M, et al. Bone-related genes expressed in advanced malignancies induce invasion and metastasis in a genetically defined human cancer model. *J Biol Chem* 2003;278:15951–7.